Electrochemical Study on Corrosion Inhibition of X52 Steel by Non-ionic Surfactant in Substitute Ocean Water

L.M. Quej-Aké[*], A. Contreras and J. Aburto

Instituto Mexicano del Petróleo. Eje Central Lázaro Cárdenas Norte 152, Col. San Bartolo Atepehuacan, C. P. 07730, México.
[*]E-mail: lquej@imp.mx

The corrosion inhibition for X52 pipeline steel exposed to substitute ocean water adding non-ionic surfactant under two hydrodynamic conditions were studied by using Reynolds number and shear stress near to laminar flow condition. Impedance and Tafel curves were used to assess the electrochemical behavior for X52 steel. Qualitative analysis shown that corrosion rate for X52 steel exposed to corrosive solution without surfactant can be attributed to the rusted by erosion process. Quantitative analysis suggests that laminar flow enhanced the corrosion inhibition for X52 steel when surfactant is added. In addition, limiting current density and adsorption process confirms that the presence of surfactant significantly decreased the corrosion rate as the flow condition also increased. Thermodynamic determination indicated that surfactant electrostatically and physically is adsorbed on X52 steel surface using laminar flow. Calcareous and chloride compounds on X52 steel surface exposed to substitute ocean water could be eliminated by using surfactant.

1. INTRODUCTION

During the transportation of crude oil as light, heavy or extra-heavy or finished product taken from tanker vessel to reach the coast through marine pipes, the fluid flow properties containing seawater are affected to different velocity profiles. Thus, it is well know that at the end of this transportation internal surfaces of the marine pipes reveals corrosion damage by rusted. Therefore, fluid flow changes are associated to low Reynolds number, Re in marine pipelines. Moreover, Re effects in crude oil-in-water and heavy crude oil-in-water emulsions is a complicated study. In addition, internal corrosion in marine pipelines taken from offshore is attributed to seawater presence. Thus, in field it is assumed that the internal corrosion for marine pipes is due to laminar flow presence. There are many studies related to this type of flow in which its velocity profile is low, named localized

corrosion such as pitting, intergranular corrosion, filiform corrosion, microbial corrosion, and stress corrosion cracking or corrosion fatigue could occur at the bottom of internal pipelines [1-30]. The another type of flow (turbulent flow), generalized corrosion can take place in all internal pipeline due to the presence of hydrocarbon-water emulsions or hydrocarbon-water-gas emulsions in presence of particles which is attributed to erosion and friction [31-37]. It is well known that the internal corrosion studies for low carbon steel exposed to different types of electrolytes in form of one, two or three phase can be complicated [35-37]. Therefore, we supposed that the corrosive solution could be minimized with the presence of turbulent flow using one phase (water and/or hydrocarbon phase), two phase (heavy and/or extra-heavy crude oil-in-water emulsions) or three phase (heavy and/or extra-heavy crude oil-in-water-gas emulsions). In addition, shear stress and Re are two dynamic properties, which can be associated to the physicochemical interaction between the metallic wall and the resistance of the fluid and the transverse velocity gradient [1,39,40]. It is well known that Reynolds number in both type of flow (laminar or turbulent flow) is associated with the pipe area (in m^2). Thus, factors determining the Reynolds number and average flow velocity of transported hydrocarbon is very complicated in oil and gas industry [41]. For engineering purposes, it is recommended that the pipe flow is laminar if the number of Re is less than 2000. A number of Re between 2000 and 4000 is considered a transition flow [4]. A turbulent flow is the system where the Re is higher than 4000 [1,4,5]. It is important to mention that, the most of the cited work in this introduction is related to corrosion of crude oil, while the title is related to simulated ocean water. Actually, the authors are trying to simulate the corrosive medium which accompany crude oil, dry and wet gas. However, they should consider that corrosive medium in oil and gas industry is a saline water containing dissolved CO_2 and H_2S acid gasses [42,43] like a sour environment for promoting sulfide film and possible carbonic acid (H_2CO_3). Thus, as a first approach to characterize the corrosion process for X52 steel in the more drastic condition (100% of water presence), substitute ocean water as representative seawater solution which is recommended by ASTM D1141 [44] was taken into account without CO_2, H_2S or H_2CO_3 acid gasses. There are three electrochemical tests in laboratory level, which is associated to hydrodynamic studies. In the first, the working electrode is moved with respect to the solution in which the fluid is forced by convective mass transport method using a rotating disk electrode (RDE) [45]. In the second, the working electrode is remained in static condition (without movement) and solution is moved by the stirrer, and the last the working electrode is moved with respect to the solution in which the fluid is forced by tangential effects on turbulent flow by using a rotating cylinder electrode (RCE), mainly [45]. In addition, an attraction on metal substrate and the formation of the oxides are expected in laminar condition by using RDE. In RCE disbonding effects of metal oxides or corrosion products in turbulent condition can occur. Thus, erosion effects by impact of particles is reached when fluid flow on internal pipe is taken into account. Therefore, the aim of this work was to investigate the Re effects and inhibition behavior of a non-ionic surfactant simulating internal corrosion process for marine pipes exposed to synthetic ocean water (taken from tanker vessel to reach the onshore). In this case, it is assumed that water phase is the more aggressive condition for internal pipelines walls. EIS and Tafel polarization studies were carried out near to laminar flow conditions in order to study Reynolds number (Re) and shear stress (τ in N/m^2). According to results, a benefical effect for the X52 in presence of surfactant and a contrary effect (dissolution of the steel) were

analyzed in the laboratory conditions here used. At the end to the electrochemical evaluation different surface images reveals that X52 steel is rusting by erosion and pitting corrosion.

2. EXPERIMENTAL

2.1. Corrosive media preparation

Substitute ocean water as a representative seawater solution was prepared according to standard test ASTM D1141 [44]. Thus, to prepare the ocean water (pH around 8.4) is necessary to weigh out (expressed in g/L): 24.53 sodium chloride (NaCl), 5.20 magnesium chloride ($MgCl_2$), 4.09 anhydrous sodium sulfate (Na_2SO_4), 1.16 calcium chloride ($CaCl_2$), 0.695 potassium chloride (KCl), 0.201 sodium bicarbonate ($NaHCO_3$), 0.101 potassium bromide (KBr), 0.027 boric acid (H_2BO_3), 0.025 strontium chloride ($SrCl_2$) and 0.003 sodium fluoride (NaF). Then, weighed amount of powders were dissolved in 1000mL of deionized water. For the electrochemical tests, a constant volume of 100 mL of substitute ocean water was used as blank. Regarding surfactant, it is an organic compound containing non-linear structures of C_9 aliphatic chain, aromatic compounds (benzene) and ethylene oxide chains with the formula C_9H_{19}-C_6H_4—$(C_2H_4O)_4$-OH which was reported in a previous work [46]. Thus, non-ionic surfactant containing ethylene oxide chains mainly, could be used as possible corrosion inhibitor.

60 mg/L surfactant was used for the corrosion inhibition study. The pH value was determined by using a pH meter; redox potential was determined using a silver/silver chloride electrode and a platinum mesh as is recommended by ASTM G200 [47]. Salinity value was obtained using a salinometer Koehler Instrument Company, Inc. Table 1 shown some of the physicochemical properties measured for substitute ocean water.

Table 1. Physicochemical properties measured for substitute ocean water used.

pH	Redox potential (mV vs Ag/AgCl)	Salinity (wt.%)
8.2	235	2.4

2.2. Cell and electrode arrangement

All electrochemical tests were carried out in an electrochemical cell with three electrodes arrangement. In the working electrode (WE), a X52 steel rotating disk electrode that contains a rod of pipeline steel with 0.5 cm^2 (0.8 cm in diameter) of area was used. WE was mechanical grinding using emery papers of grade 180, 240, 500 and 600 to obtain a flat, homogeneous and clean X52 steel surface. A rod graphite as auxiliary electrode and saturated calomel electrode (SCE) as reference electrode were used. Samples of X52 steel were analysed in order to determine their chemical composition by plasma emission and X-ray fluorescence. The material composition used in this study is shown in Table 2.

Table 2. Chemical composition of the X52 steel (wt. %)

C	Mn	Si	P	S	Cu	Cr	Ni	Nb	V	Ti	Al	Fe
0.08	1.05	0.26	0.019	0.003	0.019	0.02	0.02	0.041	0.054	0.002	0.038	Bal.

Figure 1 shows a typical microstructure of the X52 steel used in this study. Low carbon steels generally have a ferrite-perlite structure containing little dark areas of pearlite in the grain boundaries mainly, which is formed by layers of ferrite and cementite. Moreover, the most of the structure consists of light areas of ferrite with grain size of around 10 - 20 μm.
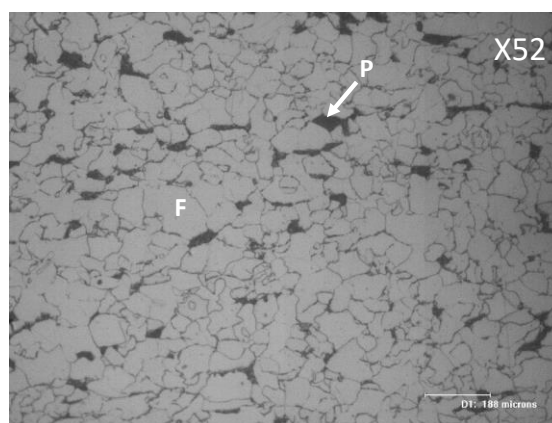
Figure 1. Typical microstructure of X52 steel obtained by optical microscopy.

2.3. Electrochemical parameter control

The electrochemical evaluation was carried out at open-circuit potential using X52 steel rotating disk electrode and magnetic stirrer; tests were performed from 0 to 2000 rpm. The temperature of evaluation was 30°C. Polarization curves were obtained by potential scanning from ±300 mV vs OCP at a sweep rate of 1 mV/s. The electrochemical impedance spectroscopy tests (EIS) were measured using 10 mV of perturbation and 10 kHz to 10 mHz of frequency after 2h of exposition of the working electrode. Taking into account EIS spectra, capacitance and resistance values were obtained from Boukamp equivalent circuit software [48]. In this manner, corrosion studies were carried out in order to correlate the corrosion resistance with different physical process such as the solution resistance (R_s), corrosion products resistance (R_{cp}), charge transfer resistance (R_{ct}) and the capacitance contribution (C) of film growth on the steel surface [48-50]. In addition, shear stress (τ in N/m^2) calculation were carried out in order to correlated with electrochemical responses.

2.4. Shear stress calculation

The shear stress values were calculated from the equation 1:

$$\tau(\frac{N}{m^2}) = 0.07951*\omega^2*\rho*\mathrm{Re}^{-0.3}*r^2 \tag{1}$$

where ω is the angular frequency rotation (angular velocity of the electrode) in rad per second, ρ is the density of the fluid in kg/cm^3, r is the radius of an electrode in m.

3. RESULTS AND DISCUSSION

3.1. Hydrodynamic parameters

Table 3. Hydrodynamic parameters for substitute ocean water at different rotation speed of the X52 steel rotating disk electrode and magnetic stirrer.

rpm	ω (rad/s)	v (m/s)	Re ($Dv\rho/\mu$)	Re ($\rho\omega r^2/\mu$)	τ (N/m^2)
0	0	0	0	0	0
200	20.94	0.08	1056	528	0.08
400	41.89	0.16	2113	1056	0.28
500	52.36	0.20	2642	1321	0.41
600	62.83	0.25	3170	1585	0.56
750	78.54	0.31	3963	1981	0.82
1000	104.73	0.41	5284	2642	1.33
1500	157.09	0.62	7926	3963	2.66
2000	209.46	0.83	10568	5284	4.34
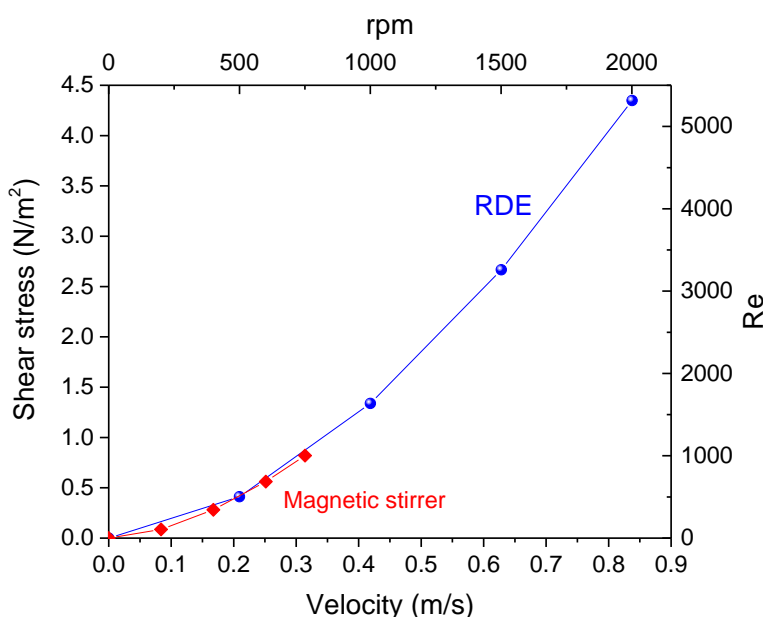
Figure 2. Hydrodynamic profiles for substitute ocean water using X52 steel rotating disk electrode and magnetic stirrer.

Table 3 shows hydrodynamic parameters obtained for the substitute ocean water at different rotation speed of the X52 steel rotating disk electrode in order to calculate Reynolds number (Re) and shear stress (τ). For substitute ocean water at 25°C the following physicochemical properties were calculated according to the methodology proposed elsewhere [51]: ρ = 1025 kg/m^3, μ = 0.00065 kg/ms, rev = π*D=0.025132741, v(m/s) = rev*π*d/s, ω(rad/s) = (rpm*360)/(57.29*60). In this case, D=0.008 m was used for X52 steel rotating disk electrode. Figure 2 show a comparison of RDE vs magnetic stirrer using some equations related to Reynolds number (Re) and shear stress (τ) [1,2].

Tebbal and Kane [1,2] performed some calculation of Re and τ using a method which is referred to simulating the distillation tower of crude oil and they proposed relations for calculation of shear stress and Re number in an autoclave without any verification with experimental data. While the simulated system in this work is just a small cell and there is no guarantee that the proposed relation with Tebbal and Kane [1,2] is applicable to pipeline systems. Thus, there is at least two major differences between these works: the type of fluid and the experimental setup. Figure 2 shows the shear stress and Re equivalencies obtained from X52 steel rotating disk electrode and magnetic stirrer. In this figure, it is possible to observe that X52 steel rotating disk electrode immersed in substitute ocean water displayed a second higher shear stress. The location of this feature (> 1.0 N/m^2) suggests the presence of laminar flow and transition flow, which is associated to corrosive condition. According to above, rotating disk electrode (RDE) is a versatile tool for understanding the mass transfer process that take place in substitute ocean water in laminar flow; meanwhile, magnetic stirrer method is only adequate for very low laminar flow studies (near to stagnant conditions). However, this analysis there is no proof that corrosive ions or surfactant is adsorbed on X52 steel surface.

According to Figure 2, it is important to note that the proposed relation for calculation of shear stress and Re number is for the study of flow in pipelines, and is not meaningful for study of flow regime around a rotating electrode and stirred flow. However, it is important to study the electrochemical behavior for X52 steel exposed to substitute ocean water.

3.2. Electrochemical impedance spectroscopy (EIS)

EIS plots for X52 steel exposed to substitute ocean water with and without surfactant (60 mg/L) surfactant using various shear stress are shown in Figure 3. The corresponding resistance and capacitance parameter measurements are summarized in Table 4. The equivalent circuit for interpretation of EIS data was taken into account from the analysis proposed elsewhere [52]. Where, C_1 and C_2 are showed in Table 4. These constant are attributed to corrosion products and double layer (or surface film growth on the steel surface), respectively [48-50].
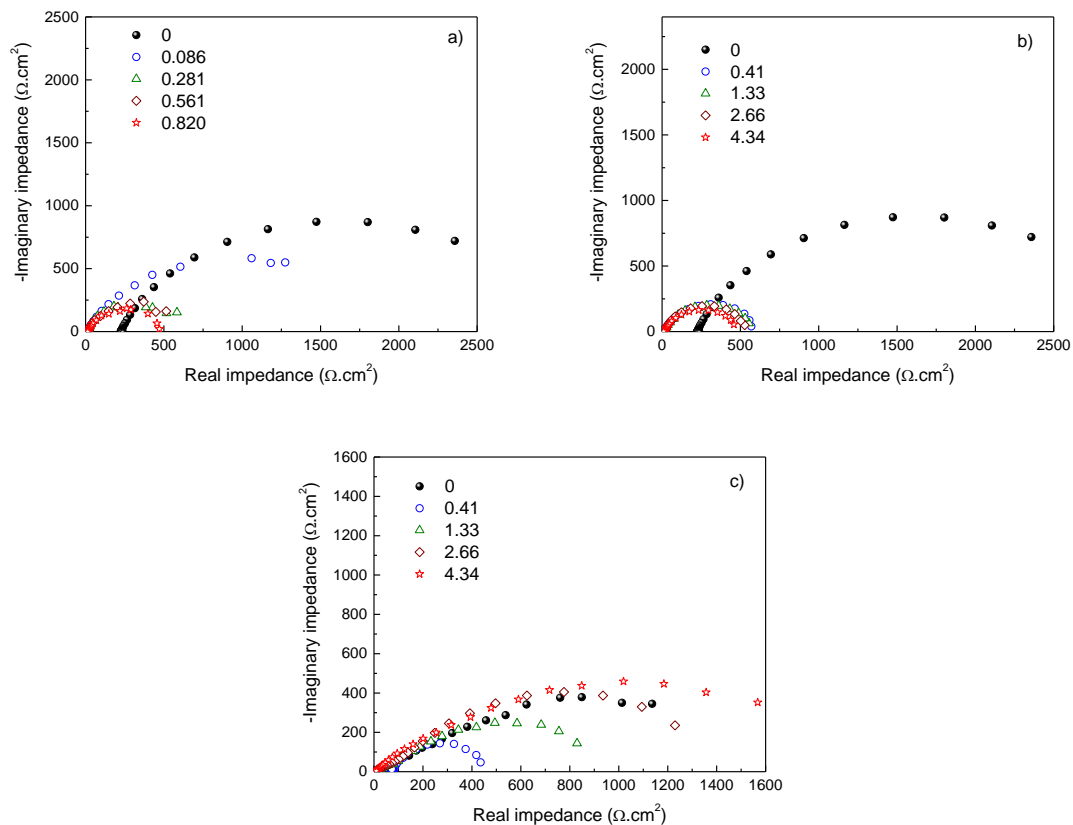
Figure 3. Nyquist diagrams for X52 steel exposed to substitute ocean water at different shear stress (τ). a) blank from magnetic stirrer, b) blank from X52 steel rotating disk electrode and c) X52 steel rotating disk electrode adding 60 mg/L non-ionic surfactant.

According to Figure 3c and Table 4, X52 steel immersed in substitute ocean water with surfactant, indicate most clearly the presence of adsorbed species at high shear stress (relative increase in the real and imaginary impedance values compared to the blank). This result suggests that the high shear stress or high Re values eliminate the presence of the possible diffusion effect and remove the corrosion products (porous, soluble and conductive deposits); meanwhile the surfactant added can block the active sites on the working electrode decreasing the corrosion rate as shear stress increases. It is important to mention that inductive effects are observed at low frequencies in which could be attributed to pitting corrosion or dissolution for X52 steel.

In addition, it is possible to note that in absence of surfactant the measured shear stress and the electrical resistance decrease; but at 0 N/m^2 the electrical resistance parameter significantly increased in which stagnant condition is generated. This is a good result and merits for further investigation by the possibility that surfactant could act as corrosion inhibitor in water media; or may be used for reduce the crude oil viscosity increasing flow by using oil-in-water emulsions [12,17,18].

Table 4. Electrochemical parameters obtained from EIS of X52 steel in substitute ocean water at different shear stress (τ) as hydrodynamic condition. The EIS spectra were fitted by using the non-linear least squares fit program of Boukamp.

rpm	τ (N/m^2)	R_s ($\Omega.cm^2$)	R_{cp} ($\Omega.cm^2$)	R_{ct} ($\Omega.cm^2$)	C_1 ($\mu F/cm^2$)	C_2 ($\mu F/cm^2$)
			Using magnetic stirrer			
0	0	225	34	3086	42	122
200	0.08	11	7.7	2089	12	161
400	0.28	10	11	584	15	399
600	0.56	10	6	690	11	519
750	0.82	12	5.6	481	30	337
		Using X52 steel rotating disk electrode				
0	0	225	34	3086	42	122
500	0.41	11	13	614	11	261
1000	1.33	10	6	610	13	170
1500	2.66	10	4	554	19	193
2000	4.34	10	2	509	14	236
		X52 steel rotating disk electrode adding 60 mg/L non-ionic surfactant				
0	0	17.2	363	1185	135	57
500	0.41	72.8	128	233	178	161
1000	1.33	10.04	371	655	136	509
1500	2.66	9.7	398	1234	131	59
2000	4.34	9.7	462	1486	128	63

3.3. Polarization curves

When conducting cathodic polarization tests in substitute ocean water using magnetic stirrer (Figure 4a), possible interference (air bubbles or oxygen presence) from the interaction between steel surface and fluid is a concern due to very low shear stress that tending to laminar flow. However, it is possible to assume that the steel surface has many additional features (components of the substitute ocean water), which may be deposited during the shear stress procedure. Thus, in Figure 4b it is possible to note that at intermediate cathodic voltages a reduction peak is observed in X52 steel rotating disk electrode system, promoting the deposit of calcareous or chloride compounds [52-54]; but, no significant cathodic and anodic current density were observed in all shear stress with X52 steel rotating disk electrode. Cathodic polarization shown that the electrochemical responses are no dependent to the shear stress. However, important displacements of current density toward lower values are observed in X52 steel rotating disk electrode when 60 mg/L non-ionic surfactant is added in substitute ocean water (Figure 4c). This result suggests that a positive effect on shear stress performance may occur when surfactant as corrosion inhibitor is taken into account [55]. Some authors [56-59] have been reported that the factors affecting the corrosion process for different API 5L steels under high hydrodynamic conditions are: the mechanism type of replacement of water molecules, interaction effects of the inhibitor with freshly generated Fe^{2+} ions, increase of inhibitor concentration, removal of inhibitor films, high shear stress (high flow velocity) effects, erosion process, among other

data. However, high shear stress can provoke metallic dissolution and high corrosion products generation (more iron rusting) promoting possible erosion process and pitting corrosion, but can also promote the mass transport of surfactant on X52 steel rotating disk electrode under moderate flow velocity (laminar flow up to 2000 rpm = 4.34 N/m^2), where a beneficial inhibition effects for X52 steel exposed to substitute ocean water can occur. Thus, a poor dissolution or little formation of iron oxides on X52 steel surface with different electric double layer attributed to corrosion inhibitor could occur [52]. The above means that the competition between the corrosive ions and the surfactant at the active sites of the X52 steel can help to dissolved the salts embedding [52].
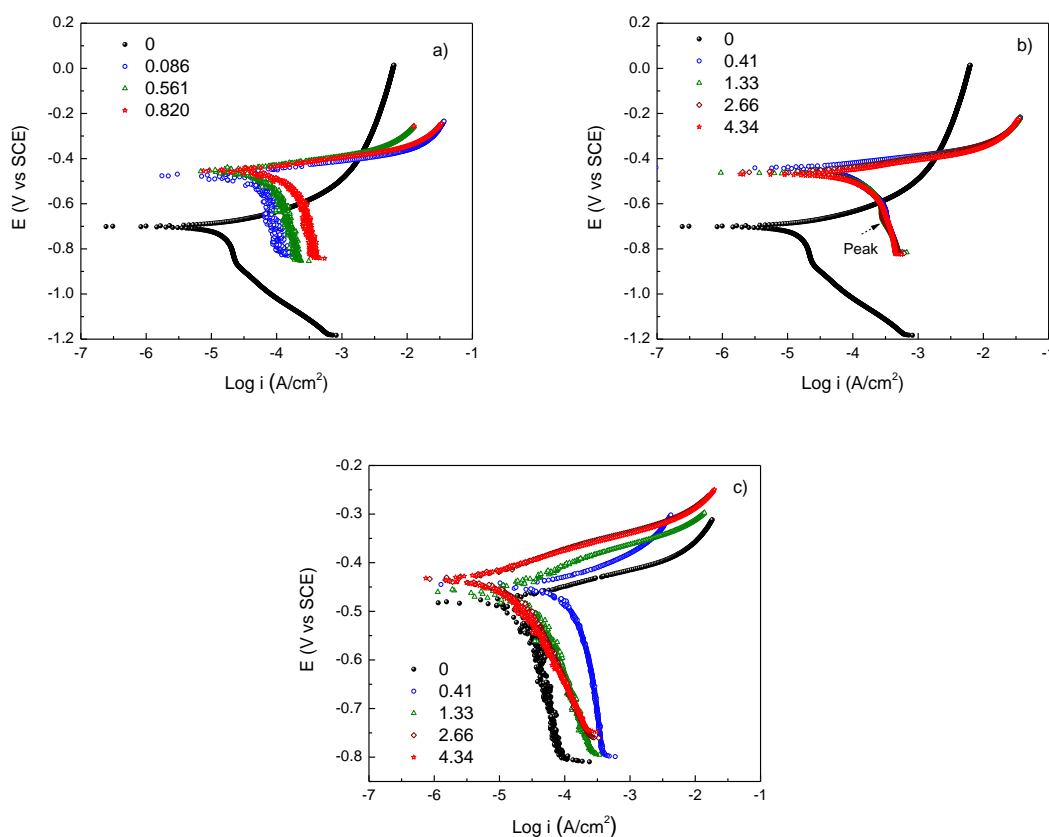
Figure 4. Polarization curves for X52 steel exposed to substitute ocean water at different shear stress (τ). a) blank from magnetic stirrer, b) blank from X52 steel rotating disk electrode and c) X52 steel rotating disk electrode adding 60 mg/L non-ionic surfactant.

Tables 5 lists electrochemical parameters calculated for X52 steel exposed to substitute ocean water and 60 mg/L non-ionic surfactant. It is observed that X52 steel rotating disk electrode without surfactant exhibited the highest corrosion rate in all shear stresses, which is agree with EIS results. In addition, positive effects of the shear stress on corrosion rate adding surfactant are obtained. This is reinforced by the corrosion rates profiles showed in Figure 5.

Table 5. Electrochemical parameters obtained from polarization curves of X52 steel exposed to substitute ocean water at different shear stress (τ).

τ (Pa)	$-E_{corr}$ (mV/SCE)	i_{corr} (A/cm^2) x 10^{-5}	β_a (mV/dec)	$-\beta_c$ (mV/dec)	CR	
					(mm/year)	(mpy)
Using magnetic stirrer					
0	700	0.88	71	1305	0.010	0.397
0.086	473	1.80	45	672	0.020	0.811
0.281	474	5.80	112	1445	0.067	2.613
0.561	453	3.27	85	265	0.037	1.443
0.820	454	6.16	58	655	0.071	2.769
Using X52 steel rotating disk electrode					
0	700	2.51	71	1304	0.029	1.131
0.41	469	5.26	74	297	0.038	1.482
1.33	439	3.20	56	216	0.037	1.446
2.66	458	3.60	59	216	0.041	1.626
4.34	462	9.82	99	258	0.113	4.438
X52 steel rotating disk electrode adding 60 mg/L non-ionic surfactant					
0	0.482	0.88	39	471	0.010	0.397
0.41	0.444	5.12	44	151	0.029	1.146
1.33	0.460	1.91	55	180	0.022	0.858
2.66	0.433	0.45	45	90	0.005	0.206
4.34	0.433	0.42	38	68	0.004	0.187
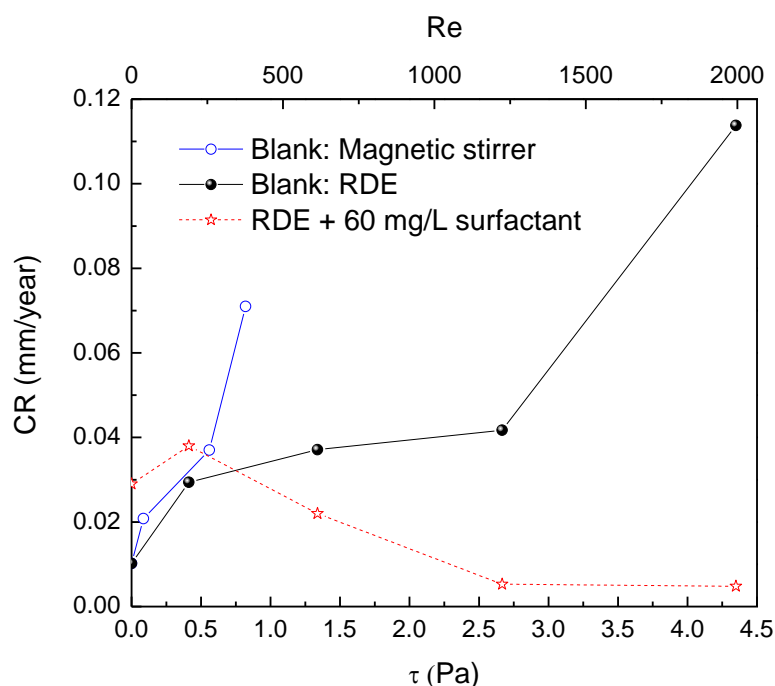
Figure 5. Corrosion rate for X52 steel exposed to substitute ocean water at different shear stress (τ) as hydrodynamic condition.

3.4. Activation and diffusion controlled reaction

According to Azghandi *et* al. [60], the electrochemical parameters calculated from Tafel polarization curves could be taking into account for analyses the activation and diffusion controlled reaction using the Levich equation. Thus, the limiting current density (i_L) is determined as a function of the angular frequency rotation ($\omega^{0.5}$) of rotating disk electrode, which is described as follow:

$$i_L = 0.62 * n * F * A * C * D^{0.666} * v^{-0.166} * \omega^{0.5}$$

(2)

Where n is the number of electrons, F is the Faraday constant, A is the area of electrode (0.5 cm^2), C is the concentration (1 mol/cm^3), D is the diffusion coefficient (0.00001 cm^2/s), v is the kinematic viscosity (0.01 cm^2/s), and ω is the angular frequency rotation. Figure 6 shows that a linear relationship is observed in X52 steel rotating disk electrode without addition of surfactant, indicating that a diffusion-controlled process and possible deterioration on steel surface may occur. However, no linear behavior is observed when 60 mg/L surfactant is added. Thus, it is possible to assume that surfactant can block the active sites and i_L values decrease as shear stress is increasing. In addition, this result suggests that a decrease diffusion-controlled process and a good corrosion inhibition could occur, which is confirmed with CR values shown in Figure 5.
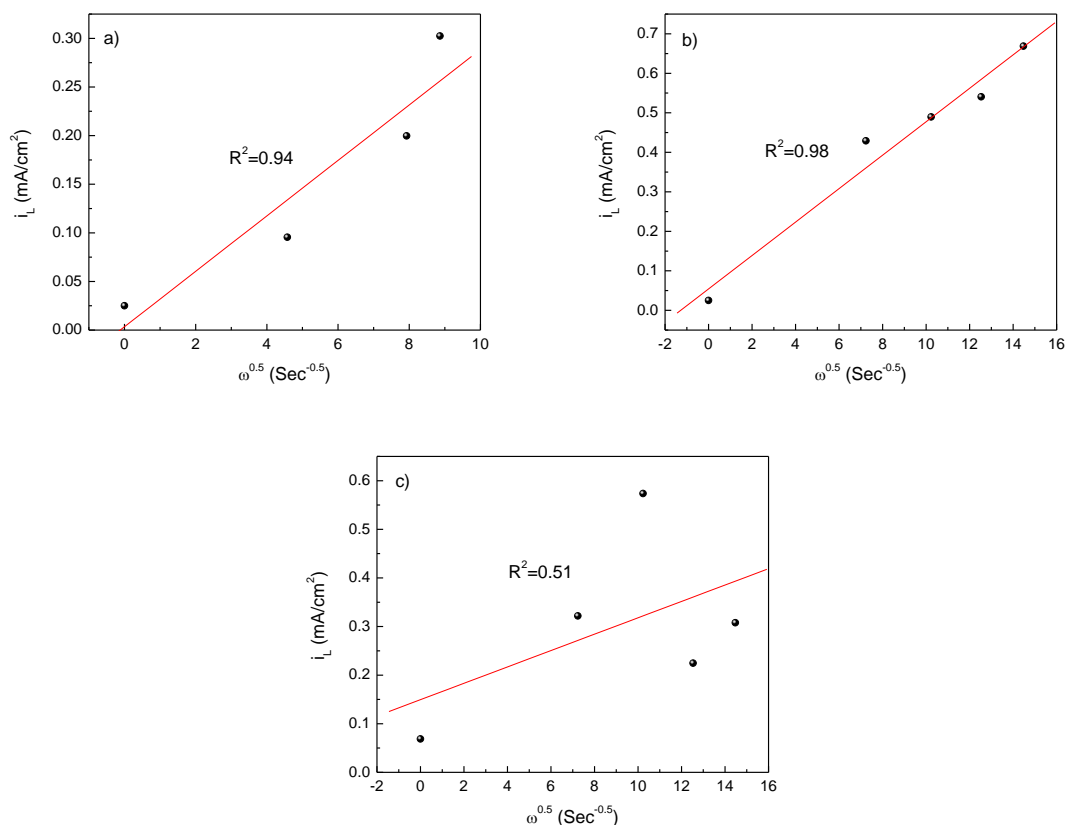
Figure 6. Levich plot for X52 steel exposed to substitute ocean water, a) With magnetic stirrer, b) X52 steel RDE, and c) X52 steel RDE adding 60 mg/L non-ionic surfactant.

3.5. Adsorption process

To understand the functionality of the surfactant as corrosion inhibitor, it is suggested focusing further effort on well-inhibited surfaces. Moreover, for corroded surfaces the interpretation of measurements is largely restricted to adsorption process using surfactant. In this manner, the concentration of surfactant ($C_{surfactant} = 0.155$ M), the degree of surface coverage of the actives sites (θ), and the thermodynamic parameters were calculated according to equations reported in previous work [61], which are associated with adsorption isotherms of Langmuir, Frumkin, Freundlich [62,63]. The hydrodynamics (Re, τ) and thermodynamic ($-\Delta G°_{ads}$, θ) parameters are showed in Table 6. Figure 7 shows the thermodynamic versus hydrodynamic parameters measurements.

Table 6. Adsorption constants and thermodynamic parameters for X52 steel RDE exposed to substitute ocean water plus 60 mg/L non-ionic surfactant at different shear stress.

τ (N/m^2)	Re	θ	ln (55.5k_{ads})	$-\Delta G°_{ads}$ (kJ/mol)
0	0	0.64	6.49	16.08
0.41	1321	0.22	4.65	11.52
1.33	2642	0.40	5.50	13.63
2.66	3963	0.87	7.80	19.34
4.34	5284	0.07	3.31	8.22

Molecular weight of non-ionic surfactant = 387 g/mol.
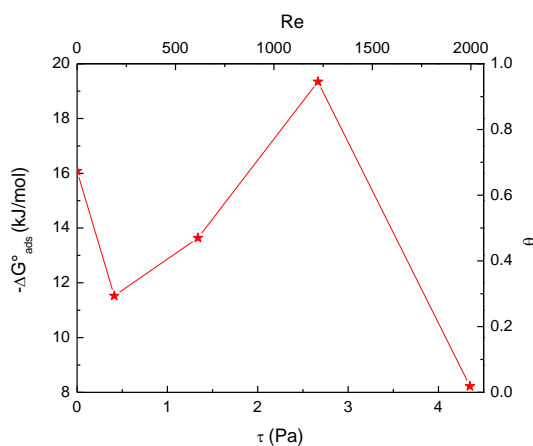
Figure 7. Thermodynamic ($-\Delta G°_{ads}$, θ) vs hydrodynamic (Re, τ) parameters in substitute ocean water with 60 mg/L non-ionic surfactant using X52 steel RDE.

Around laminar flow, the adsorption constant (k_{ads}) and $-\Delta G°_{ads}$ of X52 steel exposed to substitute ocean water with surfactant, exhibited higher values than turbulent flow. However, thermodynamic values decrease with increases in shear stress, thus the turbulent condition means that surfactant is more difficult to adsorb on X52 steel surface and consequently it provides a little

adsorption. It is important to mention that the little adsorption could also be attributed to the easy remove of carbonate or chloride compounds or any type of soluble oxide compounds when shear stress is increased. In this manner, corrosion rate can also be decrease as shear stress is increased and possible wear and erosion for steel surface can be controlled.

It is well known that a negative value of $-\Delta G^{\circ}_{ads}$ indicate that adsorption occurred spontaneously with the formation of a film strongly adsorbed on the metal surface [57-59]. Furthermore, ΔG°_{ads} around -20 kJ/mol or lower is associated with electrostatic interactions between the charged molecules and the charged metal, which indicates that a process of physical adsorption may occur [59]. In this manner, an electrostatic adsorption process may occur when 60 mg/L non-ionic surfactant is added at turbulent flow. Thus, there is clear evidence of shear stress effect on corrosion process for X52 steel exposed to substitute ocean water (Figure 7).

3.6. RDE surface after electrochemical tests

Figure 8 and 9 shows some RDE surface images after electrochemical tests showing the different corrosion products and inhibition effect on X52 steel; suggesting the formation of different oxides compounds on X52 steel surface by interaction with substitute ocean water using RDE.
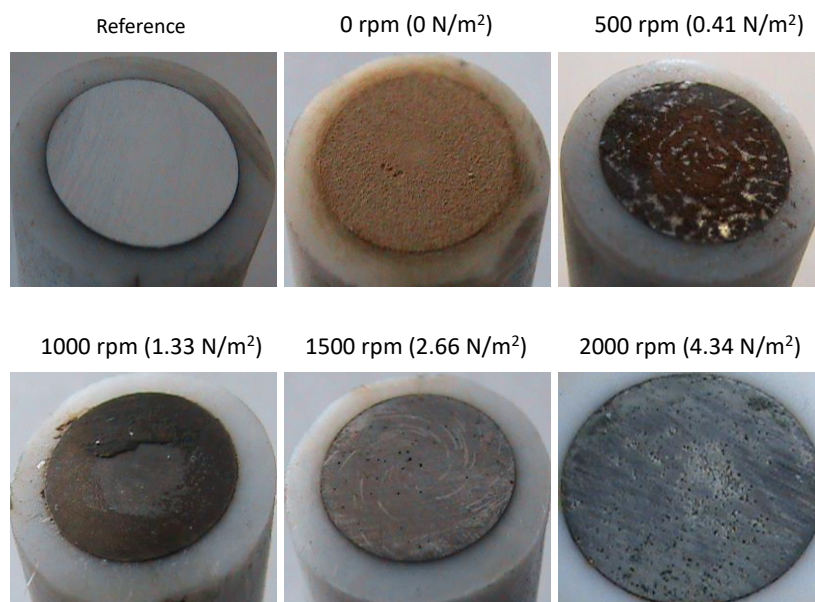
Figure 8. Images for X52 steel RDE exposed to substitute ocean water without surfactant at different shear stresses.

According to Figure 8, rusted and dark areas on X52 steel surface at 0, 500 and 1000 rpm were observed; while a high shear stresses (2.66 and 4.34 N/m^2) pitting corrosion was observed. It is important to note that the pitting corrosion process could possibly be involved in the depressed loop and the inductive effect observed at intermediate and low frequencies from Figure 3. According to Figure 9, more corrosion product were generated with addition of 60 mg/L surfactant for 0, 500, 1000

and 1500 rpm (2.66 N/m^2). However, increasing the RDE speed until 2000 rpm (4.34 N/m^2) the hydrodynamic condition reveals that X52 steel did not present rust on the surface, and the erosion and pitting corrosion were not observed adding surfactant. Thus, surfactant help to remain practically free of different corrosion process as is shown in Figure 9 at 2000 rpm.
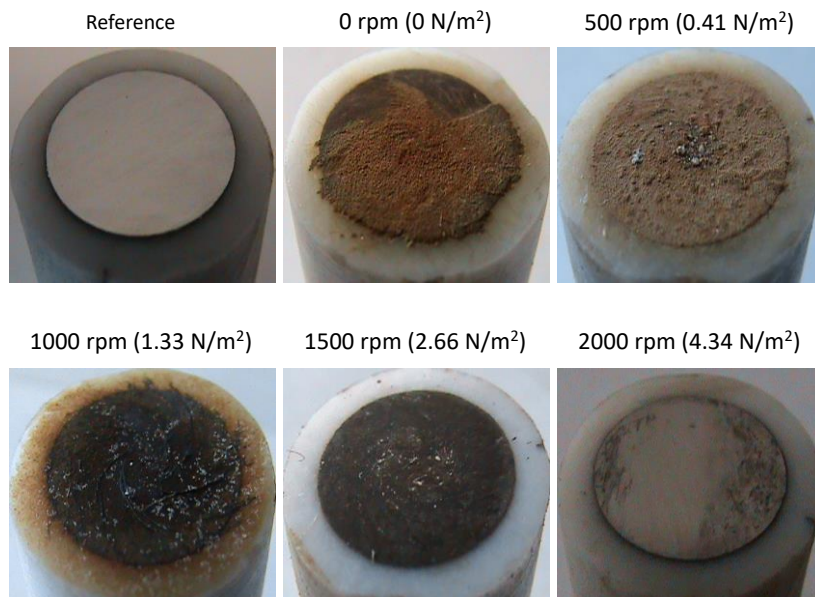
Figure 9. Images for X52 steel RDE exposed to substitute ocean water with 60 mg/L non-ionic surfactant at different shear stresses.

4. CONCLUSIONS

The corrosion inhibition for X52 steel exposed to substitute ocean water at different hydrodynamic conditions has been analysed by electrochemical tests using a rotating disk electrode. The corrosion process was analyzed at 0, 500, 1000, 1500 and 2000 rpm reaching Re values above 5000. Surfactant effect may be associate with shear stress using a rotation speed relate to the transition from lamellar and turbulent flux using the Re data. It was observed that X52 steel rotating disk electrode without surfactant exhibited the highest corrosion rate in all shear stresses, which is agree with EIS results. Meanwhile, corrosion rate has a trend to decrease adding surfactant, which is attributed to surfactant avoid contact between electroactive species and metal active sites. According to thermodynamic calculations of Gibbs free energy, the molecule is absorbed on the X52 steel surface by physisorption. Adjustment of limit current density *(i$_L$)* indicate that surfactant avoid the generation of a major current flux and high charge transfer. A low shear stresses (0, 0.41, 1.33 N/m^2) the formation of different oxides on X52 steel surface by interaction with substitute ocean water with and without surfactant was observed. A higher shear stresses (2.66 and 4.34 N/m^2) without adding surfactant the pitting attack on the steel surface was observed. However using surfactant the pitting was avoided.

References

1. S. Tebbal and R.D. Kane, *Corrosion,* 578 (1998) 1.
2. R. D. Kane and M. S. Cayard, *Hydrocarbon Processing*, 10 (1998) 97.
3. J. Czarnecki and K. Moran, *Energy and Fuels*, 19 (2005) 2074.
4. S. Nešić, G.T. Solvi and J. Enerhaug, *Corrosion,* 51 (1995) 773.
5. M.V. Azghandi, A. Davoodi, G.A. Farzi, A. Kosari, *Corros. Sci.*, 64 (2012) 44.
6. P. Bommersbach, C. Alemany-Dumont, J.P. Millet, B. Normand, *Electrochim. Acta*, 51 (2006) 4011.
7. B.R. Tian, Y.F. Cheng, *Corros. Sci.*, 50 (2008) 773.
8. D. Kuang, Y.F. Cheng, *Corros. Sci.*, 85 (2014) 304.
9. G.O. Ilevbare, G.T. Burstein, *Corros. Sci.*, 45 (2003) 1545.
10. Y.M. Zeng, J.L. Lou, P.R. Norton, *Electrochim. Acta*, 49 (2004) 703.
11. G. Engelhardt and D.D. Macdonald, *Corrosion,* 54 (1998) 469.
12. D. Örnek, A. Jayaraman, T.K. Wood, Z. Sun, C.H. Hsu, F. Mansfeld, *Corros. Sci.*, 43 (2001) 2121.
13. B.A. Abd-ElNabey, N. Khalil, M.M. Eisa and H. Sadek, *Surf. Tech.*, 20 (1983) 209.
14. V.A. Alves, A.M. Chiorcea-Paquim, A. Cavaleiro, C.M.A. Brett, *Corros. Sci.*, 47 (2005) 2871.
15. F. Mansfeld, *Electrochim. Acta*, 35 (1990) 1533.
16. A.T.A. Jenkins and R.D. Armstrong, *Corros. Sci.*, 38 (1996) 1147.
17. T.M. Watson, A.J. Coleman, G. Williams, H.N. McMurray, *Corros. Sci.*, 89 (2014) 46.
18. A.E. Hughes, J.M.C. Mol, B.R.W. Hinton, S.V.D. Zwaag, *Corros. Sci.*, 47 (2005) 107.
19. T. Wu, M. Yan, J. Xu, Y. Liu, C. Sun, W. Ke, *Corros. Sci.*, 108 (2016) 160.
20. Q. Qu, L. Wang, L. Li, Y. He, M. Yang, Z. Ding, *Corros. Sci.*, 98 (2015) 249.
21. H. Gabel, *Maters. Sci. and Eng.*, A190 (1995) 275.
22. J.R. Galvele, *Corros.*, 55 (1999) 723.
23. M. Leban, Ž. Bajt, A. Legat, *Electrochim. Acta*, 49 (2004) 2795.
24. J. Flis, M. Ziomek-Moroz, *Corros. Sci.*, 50 (2008) 1726.
25. H. Wang, E-H Han, *Electrochim. Acta*, 90 (2013) 128.
26. S.U. Koh, B.Y. Yang and K.Y. Kim, *Corrosion,* 60 (2004) 262.
27. P. Kentish, *Corros. Sci.*, 49 (2007) 2521.
28. R.W. Bosch, *Corros. Sci.*, 47 (2005) 125.
29. E.A. Charles and R.N. Parkins, *Corrosion,* 51 (1995) 518.
30. D.A. Horner, B.J. Connolly, S. Zhou, L. Crocker, A. Turnbull, *Corros. Sci.*, 53 (2011) 3466.
31. H.Q. Becerra, C. Retamoso, D.D. Macdonald, *Corros. Sci.*, 42 (2000) 561.
32. A. Rauf and E. Mahdi, *Int. J. Electrochem. Sci.*, 7 (2012) 5692.
33. T. Hong, Y.H. Sun, W.P. Jepson, *Corros. Sci.*, 44 (2002) 101.
34. H.X. Guo, B.T. Lu, J.L. Luo, *Electrochim. Acta*, 51 (2005) 315.
35. G.A. Zhang, Y.F. Cheng, *Corros. Sci.*, 51 (2009) 901.
36. X. Tnag, L.Y. Xu, Y.F. Cheng, *Corros. Sci.*, 50 (2008) 1469.
37. G.A. Zhang, Y.F. Cheng, *Corros. Sci.*, 52 (2010) 2716.
38. R. Martínez-Palou, R. Cerón-Camacho, B. Chávez, A.A. Vallejo, D. Villanueva-Negrete, J. Castellanos, J. Karamath, J. Reyes, Jorge Aburto, *Fuel* 113 (2013) 407.
39. V.V. Lagad, S. Srinivasan, R.D. Kane, *NACE Corros. Conference and Expo.*, Houston, TX, (2008) p. 08131.
40. K.D. Efird, J.L. Smith, S.E. Blevins, N.D. Davis, *NACE Corros. Conference*, The Woodlands, Texas, USA, 2004, p. 04366.

41.   E.W. McAllister, *Pipeline rules of thumb handbook*, Gulf Professional Publishing, (2002) Boston, USA.
42.   Z.F. Yin, W.Z. Zhao, Y.R. Feng and S.D. Zhu, *Corr. Eng., Sci. and Tech.*, 44 (2009) 453.
43.   R. Galvan-Martinez, J. Mendoza-Flores, R. Duran-Romero and J. Genesca-Llongueras, *J. Maters. Corros.*, 55 (2004) 586.
44.   ASTM D1141-98(2013): *Standard Practice for the Preparation of Substitute Ocean Water*.
45.   A.J. Bard and L.R. Faulkenr, *Electrochemical Methods Fundamentals and Applications*, John Wiley & Sons, (2001) New York, NY.
46.   D. Valencia, J. Aburto and I. García-Cruz, *Molecules,* 18 (2013) 9441.
47   ASTM G200-09 (2014): *Standard Test Method for Measurement of Oxidation-Reduction Potential (ORP) of Soil*, ASTM, West Conshohocken, PA
48.   B. A. Bouckamp, *Users Manual Equivalent Circuit*, Faculty of Chemical Technology, 4.51, University of Twente, (1993) Netherlands.
49.   J. R. Macdonald*, Impedance Spectroscopy*, J. W. & S., (2005) USA.
50.   A. Bonnel, F. Dabosi, C. Deslouis, M. Duprat, M. Keddam, B. Tribollet, *J. Electrochem. Soc.*, 130 (1983) 753.
51.   Mendoza-Flores, J., Kinetic Studies of CO_2 Corrosion Processes Under Turbulent Flow, *PhD Thesis*, University of Manchester, (1997) Manchester, UK.
52.   R. Pérez Campos, A. Contreras, R.A. Esparza Muñoz, *Characterisation of Metals and Alloys*, Springer International, (2016) Switzerland.
53.   Ch. Barchiche, C. Delouis, D. Festy, O. Gil, Ph. Rafait, S. Touzain, B. Tribollet, *Electrochim. Acta*, 48 (2003) 1645.
54.   R.E. Melchers, R. Jeffrey, *Corros. Sci.*, 47 (2005) 1678.
55.   M.L Free, W. Wang and D.Y. Ryu, *Corrosion,* 60 (2004) 837.
56.   P. Atempa-Rosiles, M. Días-Cruz, A. Cervantes-Tobón, J.L. González-Velázquez, J.G. Godínez-Salcedo, Y.A. Rodríguez-Arias, R. Macías-Salinas, *Int. J. Electrochem. Sci*., 9 (2014) 4805.
57.   A. Cervantes-Tobón, M. Díaz-Cruz, J.L. González-Velázquez, J.G. Godínez-Salcedo, *Int. J. Electrochem. Sci*., 9 (2014) 6781.
58.   J. Malik, I.H. Torr, W.H. Ahmed, Z.M. Gasem, M.A. Habit, R. Ben-Mansour and H.M. Badr, , *Int. J. Electrochem. Sci*., 9 (2014) 6765.
59.   A.Y. Musa, A.A.H. Kadhum, A.B. Muhamad, *Int. J. Electrochem. Sci*., 5 (2010) 1911.
60.   M.V. Azghandi, A. Davoodi, G.A. Farzi, A. Kosari, *Corros. Sci.*, 64 (2012) 44.
61.   L. Quej-Ake, A. Contreras and J. Aburto, *Int. J. Electrochem. Sci.*, 10 (2015) 1809.
62.   M.J. Rosen, *Surfactants and Interfacial Phenomena*, J. W. & S., (1989) USA.
63.   D.J. Shaw, *Introduction to Colloid and Surface Chemistry*, Butterworth Heinemann, (2000) Great Britain.